JOURNAL OF Materials CHEMISTRY

Surface-controlled growth of $LaAlO_3$ thin films by atomic layer epitaxy

Minna Nieminen,*[a] Timo Sajavaara,[b] Eero Rauhala,[b] Matti Putkonen[a] and Lauri Niinistö[a]

[a]*Helsinki University of Technology, Laboratory of Inorganic and Analytical Chemistry, P.O. Box 6100, FIN-02015 Espoo, Finland. E-mail: Minna.Nieminen@hut.fi*
[b]*Accelerator Laboratory, University of Helsinki, P.O. Box 43, FIN-00014 Helsinki, Finland*

Received 22nd March 2001, Accepted 20th June 2001
First published as an Advance Article on the web 1st August 2001

$LaAlO_3$ thin films were deposited by atomic layer epitaxy (ALE) from β-diketonate-type precursors $La(thd)_3$ and $Al(acac)_3$. Ozone was used as an oxygen source. Films were grown on soda lime glass, Si(100), MgO-buffered Si(100), sapphire and $SrTiO_3$(100) substrates. The influence of the La : Al precursor pulsing ratio on the film growth and quality in the temperature range of 325–400 °C was studied in detail. Stoichiometry and impurity levels were measured using RBS, TOF-ERDA and XPS while the chemical type of carbon impurity was identified by FTIR. XRD and AFM were used to determine crystallinity and surface morphology. The films were transparent and uniform and their thickness could be accurately controlled by the number of deposition cycles. The as-deposited films were amorphous but became crystalline upon annealing at 900 °C. The annealed films grown on Si(100) and MgO(111)-buffered Si(100) substrates had a preferred (110) orientation whereas those grown on MgO(100)-buffered Si(100) substrates showed a preferred (100) orientation. Epitaxial and smooth $LaAlO_3$ thin films were obtained on $SrTiO_3$(100) after annealing at 900 °C, verified by measurement of the X-ray rocking curve of the (200) reflection and the AFM surface roughness. Stoichiometric $LaAlO_3$ films contained <1.9 atom% carbon and about 0.3 atom% hydrogen as impurities.

Introduction

Thin films of $LaAlO_3$ have been studied mostly because of their potential use as buffer layers for the epitaxial growth of various perovskite-type films such as high temperature superconductors (HTSC), ferroelectrics and colossal magnetoresistance (CMR) oxides.[1–3] For these applications, an ideal substrate should be lattice and thermal expansion matched, chemically compatible and undergo no structural phase transitions between the film growth temperature and the operating temperature of the device.[4] For electronics applications, a low dielectric constant and low microwave losses would also be desirable.[4]

High quality HTSC films have been successfully deposited on perovskite single crystal substrates, but there is a growing demand for fabrication of HTSC films on technologically important substrates like Si, SiO_2 or sapphire. A severe interdiffusion as well as a mismatch in thermal expansion coefficients and lattice constants between these substrates and HTSC films has been the incentive to extensive studies on the growth of suitable buffer layers between substrate and HTSC films.[5] Owing to its lattice parameters and physical properties, $LaAlO_3$ is a promising candidate for a buffer layer in the deposition of various perovskite-type films. For instance, it is chemically compatible with $YBa_2Cu_3O_{7-x}$ and their lattice mismatch is small. $LaAlO_3$ has also been reported to have a reasonably low dielectric constant of 24.[6]

Thin films of $LaAlO_3$ have previously been deposited on a variety of substrates using several techniques such as metal-organic chemical vapour deposition (MOCVD),[7–9] pulsed laser deposition,[1,10] RF magnetron sputtering,[11–14] sol–gel process,[15–17] spray pyrolysis[18] and spray combustion flame technique.[19] However, there have been only a few reports on the successful deposition of $LaAlO_3$ films of high crystalline quality. Epitaxial $LaAlO_3$ films have been grown on perovskite substrates ($SrTiO_3$, $NdGaO_3$ and $LaAlO_3$),[2,3,14–16] but the use of Si, SiO_2, MgO, Al_2O_3, CeO_2 and yttria-stabilized zirconia (YSZ) as substrates has typically resulted in amorphous or polycrystalline films.[7,8,10,14,16–18] Recently, however, Molodyk *et al.*[2] and Malandrino and Fragalà[9] succeeded in obtaining highly (111) oriented $LaAlO_3$ films on YSZ(100) substrates by volatile surfactant assisted (VSA) MOCVD at 1000 °C and by thermal MOCVD at 1050 °C. Using the same technique, Molodyk *et al.*[2] were also able to grow highly (100) oriented $LaAlO_3$ films on MgO(100) at 1000 °C. Ichinose *et al.*[19] have reported the growth of (100) oriented $LaAlO_3$ films on MgO(100) by a spray combustion flame technique at 900 °C. To our knowledge, only one report exists where the growth of (100) oriented $LaAlO_3$ on Si(100) has been demonstrated. In that study[12] the as-deposited $LaAlO_3$ films grown by RF magnetron sputtering at 750 °C were amorphous. After post-annealing in oxygen at 900 °C for 30 min, the thinner films ($\sim$100 nm) had a preferred (100) orientation whereas the thicker films were randomly oriented. On the other hand, Sader[11] has demonstrated the growth of highly-textured (110) $LaAlO_3$ films on Si(100) by RF magnetron sputtering at 830 °C.

Atomic layer epitaxy (ALE),[20–22] also known as atomic layer deposition (ALD) is a thin film deposition technique utilizing gaseous precursors and chemical reactions. It can be considered as a variant of the CVD method but with the important distinction that ALE uses an alternating supply of precursors. In an ALE process of oxide materials the substrate surface is alternatively exposed to the metal precursor and the oxygen precursor separated by inert gas pulses. An excess of each precursor is supplied to saturate all the reactive surface sites leading to self-limiting growth of the film. Thus in ALE, the film growth proceeds *via* alternate surface reactions. Through its inherent surface control ALE offers several attractive features such as excellent conformality, simple and accurate thickness control and good large area uniformity, often superior to that of CVD.[23–25]

Although ALE has been used to grow several binary oxides,[20–22] so far the growth of only a few ternary oxides such

 DOI: 10.1039/b102677c

This journal is © The Royal Society of Chemistry 2001

as $LaNiO_3$,[26] $LaCoO_3$,[27] $LaMnO_3$,[28] $SrTiO_3$ and $BaTiO_3$[25] have been demonstrated. Recently, also films in the Bi–Ti–O ternary system were produced by atomic layer deposition.[29] In this paper, we report for the first time on the controlled growth of $LaAlO_3$ thin films by ALE using β-diketonates and ozone as precursors.

Experimental

Film deposition

Films were deposited in a commercial flow-type F-120 reactor manufactured by ASM Microchemistry Ltd.[20] The pressure in the reactor during deposition was 200–300 Pa. The metal precursors, $La(thd)_3$ (thd = 2,2,6,6-tetramethylheptane-3,5-dionate) and $Al(acac)_3$ (acac = pentane-2,4-dionate) were synthesized applying the method described by Eisentraut and Sievers,[30] and purified by sublimation. Ozone, used as an oxidizer, was generated from oxygen gas (99.999%) in an ozone generator (Fischer model 502). Nitrogen ($>$99.999%) obtained from a nitrogen generator (Schmidlin UHPN 3000, Switzerland) was used as a carrier and purging gas. The metal precursors were evaporated inside the reactor from an open glass crucible held at 170 and 125 °C for $La(thd)_3$ and $Al(acac)_3$, respectively. The films were grown by using the pulsing sequences shown in Table 1. To grow films with different thicknesses the number of deposition cycles was varied. The pulse times were 0.8–1.5 s for the metal precursors and 2 s for ozone while the purge times were 1–3 s. Films were deposited on soda lime glass (5×5 cm^2) and silicon (100) substrates. After optimizing the growth parameters, $LaAlO_3$ films were deposited also on sapphire, $SrTiO_3$(100) and MgO-buffered Si(100). MgO buffer layers were grown by the ALE method as described in detail earlier.[31,32] All substrates used were cleaned ultrasonically in ethanol and deionized water before use.

Selected thin film samples were heat-treated in a rapid thermal annealing furnace PEO 601 (ATV Technologie GmbH, Germany). The annealing was carried out in nitrogen atmosphere for 10–30 min at temperatures in the range 800–950 °C.

Characterization

Film thicknesses were determined by fitting the transmittance and reflectance spectra[33] measured with a Hitachi U-2000 double beam spectrophotometer in the region 190–1100 nm for silicon substrates and 370–1100 nm for soda lime glass. The surface morphology of the films was examined by a Nanoscope III atomic force microscope (Digital Instruments) operated in tapping mode (TM) with a scan rate of 1–2 Hz. To obtain representative images of the surface, wide areas (10×10 μm^2) were scanned at different parts of the sample before the scan size was reduced to 2×2 μm^2 to record the final image. Roughness values were calculated as root mean square values (rms).

Film crystallinity was measured by a Philips powder diffractometer MPD 1880 using Cu-K_α radiation. Rocking curve measurements were performed with a Bruker axs D8 Advance diffractometer using parallel beam geometry. In this study, $LaAlO_3$ is indexed assuming a pseudocubic structure although it actually has a 0.2% rhombohedral distortion.[34] However, because the difference between the rhombohedral and cubic cell is very small, the simpler cubic indexing is generally used.[2,3,14–16]

Two complementary ion beam techniques, Rutherford backscattering spectrometry (RBS) and time-of-flight elastic recoil detection analysis (TOF-ERDA) were used at the Accelerator Laboratory of the University of Helsinki to determine the film composition and stoichiometry. The lanthanum, aluminium and heavier impurity contents are readily revealed by the RBS spectra, while the amount of lighter impurities such as carbon and hydrogen are obtained more accurately from the TOF-ERDA analysis. The La : Al content ratios were determined by RBS from the ratios of the elemental yields. Statistical errors contribute to the uncertainties in RBS results, but systematic errors, such as uncertainties in stopping powers, are cancelled out. The uncertainties in the impurity contents determined by TOF-ERDA are due to statistical and possible systematic errors (stopping power uncertainties). The resulting uncertainties fall below 0.1 atom% units for contents below 1 atom% and below 0.2 atom% for contents above 1 atom%.

The RBS experiments were carried out with $^4He^+$ ions from a 2.5 MV Van de Graaff accelerator operated at 2.0 MeV. A scattering angle of 170° was used. A beam of $^{197}Au^{9+}$ ions at 48 MeV for TOF-ERDA was obtained from a 5 MV tandem accelerator EGP-10-II. The sample surface was tilted 20° and recoils were detected at an angle of 40° with respect to the incoming beam.

La and Al contents were also determined with a Philips PW 1480 X-ray fluorescence spectrometer equipped with a Rh X-ray tube. Data analysis was performed with the UNIQUANT 2.5 program, which utilises the DJ Kappa model to calculate the composition and mass thickness of an unknown bulk or thin film sample.[35] The XRF results were calibrated by plotting the XRF La/Al-ratio against the La/Al-ratio measured by RBS.

X-Ray photoelectron spectroscopy (XPS) measurements were performed at the HUT Center for Chemical Analysis with a Kratos Analytical AXIS 165 spectrometer using monochromated Al-K_α radiation. The X-ray tube voltage of 12.5 kV and current of 8 mA were kept constant throughout the analyses. Samples were measured from the surface without sputter cleaning, since ion bombardment is known to easily degrade chemical information. For surface elemental concentrations, wide binding energy spectra of 0–1100 eV were recorded at 80 eV analyser pass energy and a 1 eV step. For surface chemical analysis, high resolution regional spectra of La 3d, Al 2p, O 1s and C 1s were also collected using a 20 eV analyser pass energy and 0.1 eV steps. The charge build-up due to the insulating sample matrix was neutralized during the data acquisition with slow thermal electrons. Afterwards, the binding energy scale was corrected in the high resolution spectra, using the C–C bond in C 1s signal at 285.0 eV as an internal standard.[36]

The deposited $LaAlO_3$ films were also analyzed by FTIR spectroscopy. The transmission spectra of the films deposited on Si(100) substrates were collected with a Nicolet Magna-IR 750 equipped with a deuterated-triglycine sulfate (DTGS) detector.

Table 1 Pulsing sequences of the starting materials for the preparation of La–Al–O films. The number of deposition cycles (*N*) was varied depending on the desired film thickness

Sample	Pulsing sequence
1	$N \times [1 \times (La(thd)_3 + O_3) + 2 \times (Al(acac)_3 + O_3)]$
2	$N \times [1 \times (La(thd)_3 + O_3) + 1 \times (Al(acac)_3 + O_3)]$
3	$N \times [3 \times (La(thd)_3 + O_3) + 2 \times (Al(acac)_3 + O_3)]$
4	$N \times [7 \times (La(thd)_3 + O_3) + 4 \times (Al(acac)_3 + O_3)]$
5	$N \times [2 \times (La(thd)_3 + O_3) + 1 \times (Al(acac)_3 + O_3)]$
6	$N \times [5 \times (La(thd)_3 + O_3) + 2 \times (Al(acac)_3 + O_3)]$
7	$N \times [3 \times (La(thd)_3 + O_3) + 1 \times (Al(acac)_3 + O_3)]$
8	$N \times [5 \times (La(thd)_3 + O_3) + 1 \times (Al(acac)_3 + O_3)]$

Results and discussion

As-deposited films

The deposition temperatures of binary oxides La_2O_3 and Al_2O_3 determine the temperature range available for the growth of $LaAlO_3$ ternary oxide. Our earlier study[37] on the ALE growth

of La_2O_3 films indicated that above 300 °C self-limited film growth is achieved leading to uniform films. Above 425 °C, however, a CVD-type growth was observed and controlled deposition was no longer feasible. A study of the ALE growth of Al_2O_3 films at 250–450 °C showed that the growth is very similar to the ALE growth of Ga_2O_3 films.[38] A narrow plateau of self-limited ALE growth was observed in the temperature range 350–380 °C. Above 380 °C the growth rate increased with temperature while it decreased below 350 °C. However, the films were uniform also outside the ALE window up to 400 °C. At 300 °C the growth rate was very low and below 300 °C no film was detected. TOF-ERD analysis of a film deposited at 350 °C showed that the film was stoichiometric Al_2O_3. Therefore, based on the data of the constituent oxides, a deposition temperature range of 325–400 °C was chosen for the present study.

The film growth rates at different deposition temperatures were found to be constant at low La : Al pulsing ratios, see Fig. 1. In theory, the growth rate of a ternary oxide depends on the growth rates of the two constituent binary oxides. However, a decrease in the $LaAlO_3$ growth rates with an increase of the relative number of $La(thd)_3/O_3$ cycles was observed, as shown in Fig. 1 (inset). At higher La : Al pulsing ratios a small increase in the growth rate was detected. One possible explanation for the observed phenomenon is that the Al–O layer diminishes the growth rate of the following La–O layer. Possibly, the surface sites available are not favourable for the adsorption of $La(thd)_3$. It is also possible that the bonding mode of $La(thd)_3$ on Al–O surface differs from that on the La–O surface. Confirmation of these hypotheses would, however, require further studies.

The film composition was varied by altering the ratio of La : Al precursor pulsing cycles at different deposition temperatures, see Fig. 2. The optimum pulsing ratio was 1.75–2.0 in the deposition region 350–375 °C which resulted in a La : Al atomic ratio of about 1. Fig. 2 shows also that at lower deposition temperatures the La : Al ratios were all higher than those of the films deposited at higher temperatures. Nevertheless, stoichiometric $LaAlO_3$ films can be grown at deposition temperatures between 325 and 400 °C by carefully selecting the La : Al precursor pulsing ratio.

The deposition of the La–Al–O films was very reproducible. All the films with different La : Al atomic ratios exhibited good thickness uniformity both along and across the gas flow direction. The growth rate of stoichiometric $LaAlO_3$ film on silicon substrate was linear, as shown in Fig. 3, being 0.36 and 0.39 Å per cycle at 350 and 375 °C, respectively. The film growth rates on soda lime glass substrates were the same as on silicon substrates, the measured values being 0.35 Å per cycle at 350 °C and 0.38 Å per cycle at 375 °C. XRF measurements showed that the La : Al atomic ratio remained constant over

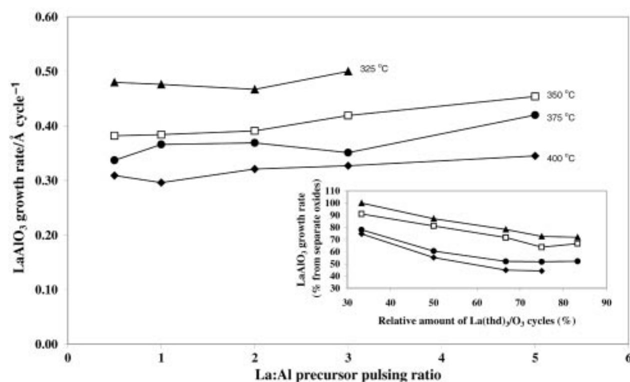

Fig. 1 The growth rate of $LaAlO_3$ films as a function of the pulsing ratio of $La(thd)_3/O_3$ to $Al(acac)_3/O_3$.

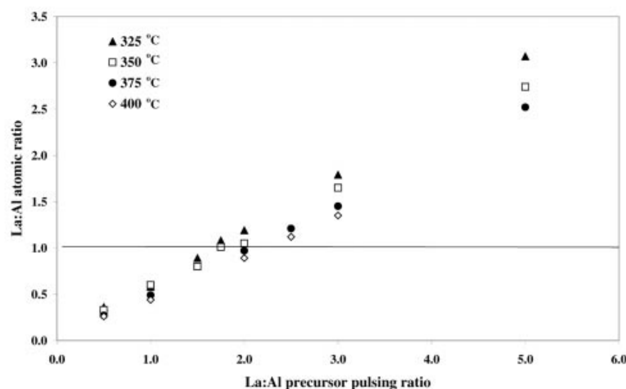

Fig. 2 La : Al atomic ratio in $LaAlO_3$ films deposited at temperatures between 325 and 400 °C on silicon(100) substrates as a function of the $La(thd)_3/O_3$ to $Al(acac)_3/O_3$ cycle ratio. The film composition was measured by X-ray fluorescence and independently verified by Rutherford backscattering spectrometry (RBS).

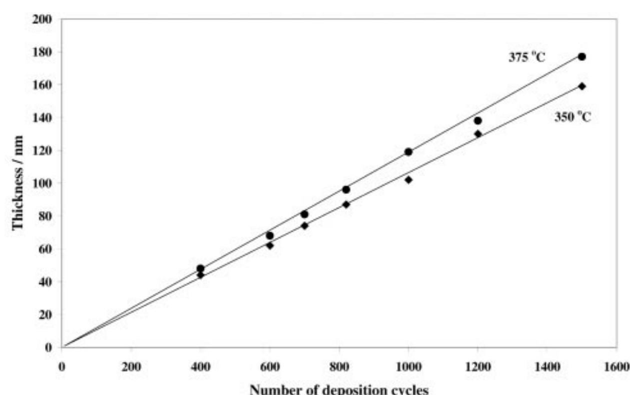

Fig. 3 Dependence of the $LaAlO_3$ film thickness on the number of deposition cycles at 350 and 375 °C. The films were grown on silicon(100).

the area of two substrates, *i.e.* $10 \times 5\ cm^2$. Also, the composition of the films was maintained even when the thickness was changed, thus indicating that the growth was well controlled.

The impurities in the $LaAlO_3$ films deposited onto Si(100) at various temperatures with a La : Al pulsing ratio of 2.0 were analyzed by TOF-ERDA. The films were found to contain small amounts of carbon, hydrogen and fluorine. Carbon was evenly distributed throughout the films and the FTIR spectra suggest that it is mainly present as a carbonate-type impurity; a similar type of carbonate impurity was recently found in ALE-grown La_2O_3 and Y_2O_3 thin films.[37,39] The films with a stoichiometric La : Al atomic ratio contained 0.8–1.9 atom% carbon and about 0.3 atom% hydrogen. A decrease in carbon impurity level from 2.4 to 0.8 atom% and also in the hydrogen impurity level from 0.5 to 0.1 atom% was observed when the deposition temperature was increased from 325 to 400 °C. At the same time, the La : Al atomic ratio decreased, indicating that carbon and hydrogen contents are mainly related to the La–O part of the film. The observed fluorine content (0.2–0.7 atom%) is caused by the Teflon gaskets or perfluorinated vacuum greases used.[39]

The surface elemental composition of the as-deposited film was determined from XPS survey scans. Only lanthanum, aluminium, oxygen, carbon and fluorine were detected. As the samples were measured without *in situ* cleaning, both carbon and oxygen species were present as contaminants at the film surface. The overall carbon content (16–30 atom%) was of the same order as surface carbon recorded for air-exposed oxide surfaces.[40] The low increase in the background intensity of the F 1s peak[41] indicated that fluorine was present as surface a contaminant.

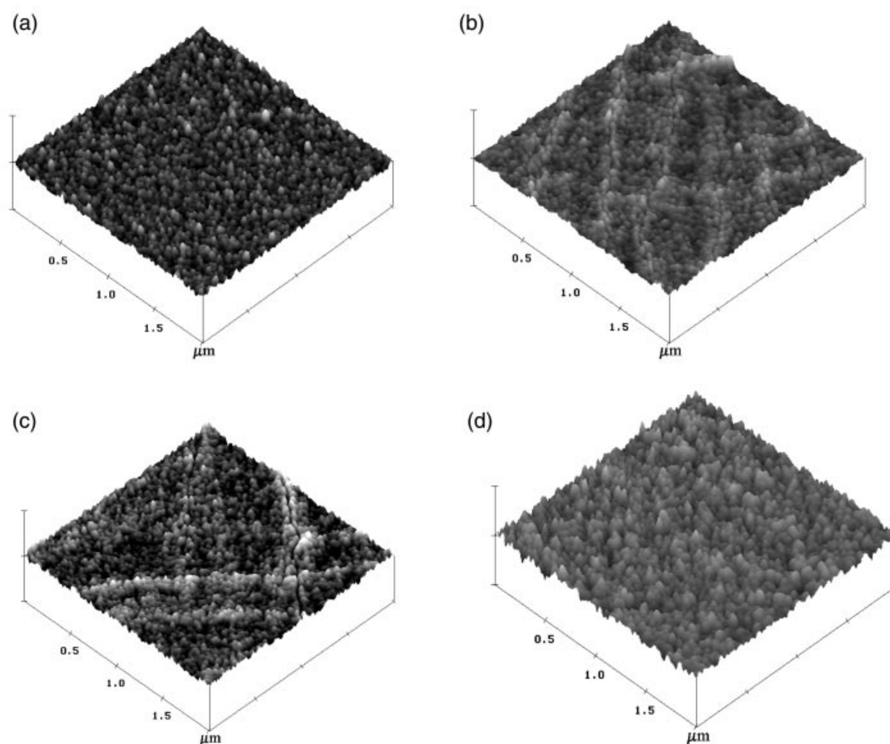

Fig. 4 AFM images of the $LaAlO_3$ thin film surfaces. Images (a)–(c) depict specimens of 75 nm film thickness grown on silicon (100) while (d) shows an image of a 135 nm thick film deposited on $SrTiO_3$(100). (a) As-deposited amorphous film, rms = 0.4 nm, (b) annealed at 900 °C in N_2 for 30 min, rms = 0.9 nm, (c) annealed at 950 °C in N_2 for 30 min, rms = 0.9 nm and (d) epitaxial $LaAlO_3$ film on $SrTiO_3$(100), rms = 1.1 nm. Image size: 2 μm × 2 μm. Depth scale: 20 nm from black to white.

For a more detailed chemical analysis, the high-resolution XPS spectra of the main constituents were also recorded. The binding energies of La $3d_{5/2}$ at 835.3 ± 0.5 eV and Al 2p at 73.4 ± 0.3 eV were in good agreement with values reported in the literature for $LaAlO_3$.[42,43] The La $3d_{5/2}$ and $3d_{3/2}$ core-level peaks were both split into two components as reported for La_2O_3, $LaAlO_3$ and other mixed oxides of lanthanum.[42–44] The oxygen signal (O 1s) consisted of two resolvable components. The broad, minor component of O 1s at 531.6 ± 0.5 eV agrees well with the tabulated values of adsorbed O^- and OH^- groups, often detected on air-exposed oxide surfaces. The main component of O 1s at 529.9 ± 0.5 eV is characteristic for O^{2-} in oxide lattice and is in good accordance with the reported values for $LaAlO_3$.[42,43]

All films grown on soda lime glass substrates were highly transparent in the wavelength region 370–1100 nm, regardless of the deposition temperature. Refractive indices of the stoichiometric $LaAlO_3$ films deposited at 350 and 375 °C were around 1.85 (at 580 nm). When the La : Al atomic ratio in the films decreased also the refractive indices of the films decreased toward 1.73 for films with La : Al atomic ratio around 0.3. Similarly, a small increase in the refractive index up to 1.9 was detected on films with La : Al ratio above 1.0. AFM measurements showed that the $LaAlO_3$ films grown on silicon (100) were smooth, as verified by the measured roughness values which were around 0.4 nm, see Fig. 4(a).

The as-deposited films on all substrates were amorphous. Therefore post-annealing was needed to obtain crystalline $LaAlO_3$ films. For these studies stoichiometric $LaAlO_3$ films were deposited on Si(100), MgO-buffered Si(100), sapphire and $SrTiO_3$(100) substrates using the optimized growth parameters at 350 and 375 °C.

Annealed films

Silicon(100) substrate. Annealing at 900 °C and above was needed to crystallize the films since all films annealed at 800 or 850 °C were still amorphous. Annealing at 900 °C in N_2 for 10 min produced polycrystalline $LaAlO_3$ films. When the annealing time was increased to 30 min and slow heating and cooling rates of 1 °C min^{-1} in the temperature range 700–900 °C were used, the resulting polycrystalline $LaAlO_3$ film had a preferred (110) orientation as indicated by the XRD pattern in Fig. 5.

Interdiffusion of the silicon substrate and the lanthanum aluminate film at temperatures around 1000 °C and above has been reported in the literature.[7,8,10] The same phenomenon was seen in our study when the annealing temperature was raised to 950 °C. According to RBS data, the elemental composition changed with depth for the film annealed at 950 °C. On the surface of the film (within approx. 40% of film thickness) a nearly stoichiometric $LaAlO_3$ phase was detected. When compared to the as-deposited film, there was a decrease in the La/Al elemental ratio from 1.05 ± 0.03 to 0.88 ± 0.03, indicating a decrease in the lanthanum content on the surface of the film. Below the surface layer, a decrease in the aluminium

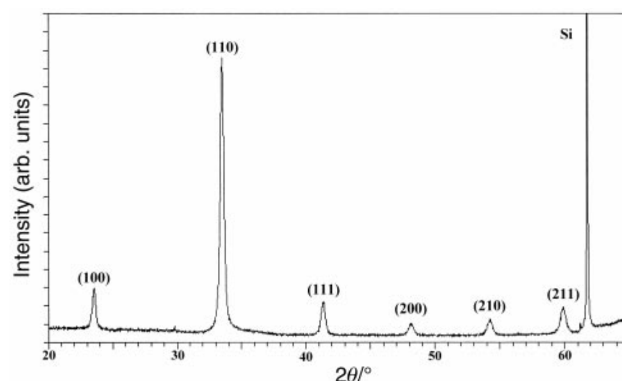

Fig. 5 XRD pattern of a 135 nm thick $LaAlO_3$ film grown on Si(100) substrate and annealed at 900 °C in N_2 for 30 min. All peaks can be indexed as those of pseudocubic $LaAlO_3$.

content and an increase in the silicon content was observed. At the film-substrate interface (within approx. 20% of film thickness) only La, Si and O were detected.

The XRD pattern of a film annealed at 950 °C contained peaks of the $LaAlO_3$ phase and also new peaks which were difficult to unambiguously identify. In our recent study on the ALE growth of $LaGaO_3$ films on silicon,[45] the formation of $La_4Ga_2O_9$ phase rather than the expected $LaGaO_3$ phase was detected when the films were annealed at 850 °C or above. The X-ray diffraction pattern of $La_4Ga_2O_9$ is very similar to that of a new phase seen in the XRD pattern of the La–Al–O film annealed at 950 °C. Unfortunately, the XRD pattern of $La_4Al_2O_9$ phase has not been reported. According to Yamane *et al.*[46] and Dohrup *et al.*[47] the crystal structures of $RE_4Ga_2O_9$ are isostructural with $Re_4Al_2O_9$ (RE = rare earth). Therefore we believe that the new phase is $La_4Al_2O_9$.

The surface chemistry of the films annealed at 900 and 950 °C was studied with XPS. In wide binding energy spectra, the same constituents were seen as for the as-deposited film. Furthermore, the high-resolution regional spectra showed that the binding energies of the La $3d_{5/2}$ and Al 2p lines remained unaffected by annealing. However, a small change in the shape of La $3d_{5/2}$ and $3d_{3/2}$ peaks was detected in both of the annealed films, indicating subtle changes in the valence band configuration which could be due to changes in the La coordination number before and after annealing, as discussed by Burroughs *et al.*[44] As for the atomic concentrations in the topmost surface regions, the film annealed at 900 °C had an La : Al atomic ratio similar to that of the as-deposited one; however, the film annealed at 950 °C had a clearly lower La : Al ratio. This result is consistent with the RBS data.

The surface morphology of films grown on Si(100) substrate and annealed at 900 and 950 °C was analyzed by AFM. Both films had a smooth surface with a surface roughness of about 0.9 nm. The annealed $LaAlO_3$ films grew in a columnar manner with a bright grain boundary region as seen in Fig. 4(b) and (c). Deep cracks were seen on the surface of a film annealed at 950 °C. Cracking has been reported in other studies of $LaAlO_3$ thin film growth on Si(100) as well.[8,10] Recently, Carlson *et al.*[1] found also similar type of cracking in the $LaAlO_3$ films when grown on $SrTiO_3/CeO_2$/Ni substrates.

MgO-buffered silicon(100) substrate. Our interest in using MgO-buffered Si(100) substrates was to study whether the ALE-grown MgO buffer layer can prevent the interdiffusion between the silicon substrate and the $LaAlO_3$ film. Molodyk *et al.*[2] obtained highly (100) oriented $LaAlO_3$ films on MgO(100) and Cabañas *et al.*[7] reported that they were able to grow highly homogeneous and compact $LaAlO_3$ films without a reaction with the MgO substrate even at a high annealing temperature of 1250 °C.

The MgO buffer layers have either a preferred (100) or (111) orientation.[31,32] The as-deposited $LaAlO_3$ films grown on MgO-buffered silicon were stoichiometric and amorphous. The films became crystalline after annealing in nitrogen flow at 900 °C for 10 min. Thinner $LaAlO_3$ films (<100 nm) grown on (100) or (111) oriented MgO had (100) or (110) preferred orientations, respectively; see the XRD patterns in Fig. 6. Thicker $LaAlO_3$ films and the films annealed with a longer period of time were randomly oriented.

When the annealing temperature was raised to 950 °C the same new peaks seen in the XRD patterns of films grown on Si(100) and annealed at 950 °C were detected, indicating the formation of the $La_4Al_2O_9$ phase. This phenomenon was most obvious when the thickness of the MgO layer or that of the $LaAlO_3$ film was below 100 nm.

Sapphire substrate. Polycrystalline $LaAlO_3$ films, with the (110) reflection being the most intense, were obtained when the films deposited on sapphire substrates were annealed at 900 °C in a nitrogen flow. Increasing the annealing time from 10 to 30 min did not have any effect on the crystal orientation. Probably, the large structural mismatch between sapphire and lanthanum aluminate results in polycrystalline films.

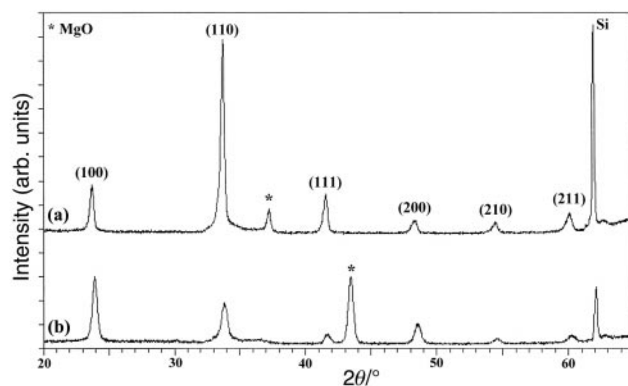

Fig. 6 XRD patterns of films grown on (a) MgO(111)-buffered Si(100) and (b) MgO(100)-buffered Si(100). The $LaAlO_3$ film thickness is 75 nm and the MgO buffer layer thickness is 140 nm. Miller indices of the pseudocubic $LaAlO_3$ are given.

$SrTiO_3$ substrate. $LaAlO_3$ films were also grown on a perovskite-type substrate, $SrTiO_3$(100). The as-deposited films were amorphous but became crystalline upon annealing at 900 °C in nitrogen flow for 10–30 min. The degree of crystallinity was enhanced when a longer annealing time and slower heating and cooling rates were used. Fig. 7 shows the XRD pattern of the $LaAlO_3$ film grown on $SrTiO_3$(100) and annealed at 900 °C for 30 min. The three peaks observed, in addition to the (100), (200) and (300) $SrTiO_3$ reflections, can be identified as being the (100), (200) and (300) reflections of the $LaAlO_3$ perovskite structure. A rocking curve scan of the (200) $LaAlO_3$ reflection is shown in the inset of Fig. 7. The full-width at half-maximum (FWHM) value of 0.119° proves that the $LaAlO_3$(100) film on $SrTiO_3$(100) is of high quality and epitaxial. Furthermore, the surface roughness was only 1.1 nm, as determined by AFM, see Fig. 4(d).

The best samples of perovskite $LaAlO_3$ films were obtained on perovskite $SrTiO_3$ substrates. This is not surprising and has also been reported in other studies.[2,14,16] Epitaxial growth of $LaAlO_3$ is achieved on lattice-matched substrates but non-lattice matched substrates will give rise to randomly or slightly oriented films. On the other hand, the (100) oriented $LaAlO_3$ films are also promising as buffer layers for the deposition of various perovskite films since such a buffer layer may change the preferred orientation of perovskite growth from polycrystalline or slightly textured to epitaxial.[2] Therefore the

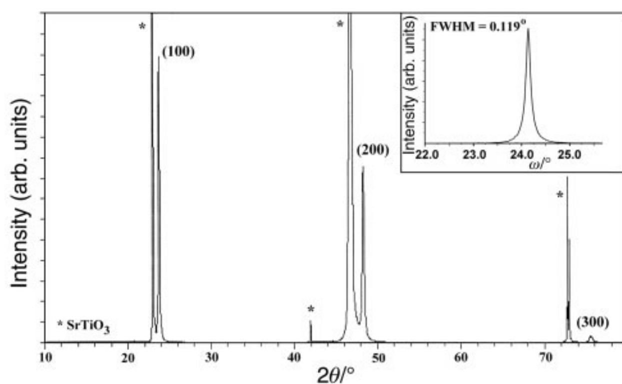

Fig. 7 XRD pattern of an epitaxial $LaAlO_3$ film grown on $SrTiO_3$(100). The film was 135 nm thick and was annealed at 900 °C in N_2 for 30 min. The inset shows the rocking curve of the (200) reflection of $LaAlO_3$ (FWHM = 0.119°).

annealing procedure of the films grown on MgO(100)-buffered Si(100) substrates as well as the effect of MgO layer thickness on the $LaAlO_3$ film quality will be studied in more detail in the future.

Conclusions

We have demonstrated for the first time the ALE growth of $LaAlO_3$ thin films on various substrates, namely Si(100), soda lime glass, sapphire, $SrTiO_3$ and MgO-buffered Si(100) using β-diketonate-type precursors for metals and ozone for oxygen. Some of the advantages of the ALE method, *e.g.* excellent control of stoichiometry, thickness and uniformity over large area substrates, are also demonstrated in this study. It is shown that stoichiometric $LaAlO_3$ films can be obtained at deposition temperatures between 325 and 400 °C by a correct selection of the La : Al precursor pulsing ratios.

The film growth was very reproducible and the films were uniform with only small thickness variations of 1–5% over the substrate area of 10×5 cm^2. A linear dependence of the film thickness on the number of deposition cycles was observed indicating a typical self-limiting ALE growth. Also the film stoichiometry was maintained with the increasing thickness, thus verifying excellent control of the process. The stoichiometric $LaAlO_3$ films contained <1.9 atom% carbon and about 0.3 atom% hydrogen as impurities.

The as-deposited films were amorphous but crystallized upon annealing at 900 °C in a nitrogen flow. By a proper selection of annealing times as well as heating and cooling rates, preferred (110) orientation was obtained in films grown on Si(100) and MgO(111)-buffered Si(100) substrates whereas films grown on MgO(100)-buffered Si(100) substrates showed preferred (100) orientation. When the annealing temperature was raised to 950 °C an interdiffusion between silicon substrate and $LaAlO_3$ film occurred.

High quality, epitaxial and smooth $LaAlO_3$ thin films were obtained on $SrTiO_3$(100) after annealing at 900 °C, verified by the X-ray rocking curves of the (200) reflection having full-width at half-maximum (FWHM) of 0.119° and by the AFM surface roughness of 1.1 nm.

Acknowledgements

The authors wish to thank Dr Joseph Campbell and Dr Leena-Sisko Johansson from the HUT Center for Chemical Analysis for performing the XPS measurements and aiding with the interpretation of the XPS data. Thanks are also due to Mr Jaakko Niinistö from Helsinki University of Technology for the AFM measurements. Mr Antti Niskanen from the University of Helsinki is thanked for the rocking curve measurements.

References

1 C. M. Carlson, J. C. Price, P. A. Parilla, D. S. Ginley, D. Niles, R. D. Blaugher, A. Goyal, M. Paranthaman, D. M. Kroeger and D. K. Christen, *Physica C*, 1998, **304**, 82.
2 A. A. Molodyk, I. E. Korsakov, M. A. Novojilov, I. E. Graboy, A. R. Kaul and G. Wahl, *Chem. Vap. Deposition*, 2000, **6**, 133.
3 G. Malandrino and I. L. Fragalà, *Chem. Mater.*, 1998, **10**, 3765.
4 M. Leskelä, H. Mölsä and L. Niinistö, *Supercond. Sci. Technol.*, 1993, **6**, 627.
5 J. Qiao and Y. Yang, *Mater. Sci. Eng.*, 1995, **R14**, 157.
6 T. Konaka, M. Sato, H. Asano and S. Kubo, *J. Supercond.*, 1991, **4**, 283.
7 M. V. Cabañas, C. V. Ragel, F. Conde, J. M. Gonzáles-Calbet and M. Vallet-Regí, *Solid State Ionics*, 1997, **101–103**, 191.
8 G. Malandrino, A. Frassica and I. L. Fragalà, *Chem. Vap. Deposition*, 1997, **3**, 306.
9 G. Malandrino and I. L. Fragalà, *Electrochem. Soc. Proc.*, 1997, **97–25**, 844.
10 V. Sandu, J. Jaklovszky, D. Miu, D. Drăgulinescu, C. Grigoriu and M. C. Bunescu, *J. Mater. Sci. Lett.*, 1994, **13**, 1222.
11 E. Sader, *Supercond. Sci. Technol.*, 1993, **6**, 547.
12 X. F. Meng, F. S. Pierce, K. M. Wong, R. S. Amos, C. H. Xu, B. S. Deaver Jr. and S. J. Poon, *IEEE Trans. Magn.*, 1991, **27**, 1638.
13 E. Sader, H. Schmidt, K. Hradil and W. Wersing, *Supercond. Sci. Technol.*, 1991, **4**, 371.
14 A-E. Lee, C. E. Platt, J. F. Burch, R. W. Simon, J. P. Goral and M. M. Al-Jassim, *Appl. Phys. Lett.*, 1990, **57**, 2019.
15 S. S. Shoup, M. Paranthaman, D. B. Beach, E. D. Specht and R. K. Williams, *J. Mater. Res.*, 1997, **12**, 1017.
16 M. F. Ng and M. J. Cima, *J. Mater. Res.*, 1997, **12**, 1306.
17 P. Peshev and V. Slavova, *Mater. Res. Bull.*, 1994, **29**, 255.
18 H. Ichinose, H. Katsuki and M. Nagano, *J. Cryst. Growth*, 1994, **144**, 59.
19 H. Ichinose, Y. Shiwa and M. Nagano, *Jpn. J. Appl. Phys.*, 1994, **33**, 5907.
20 T. Suntola, *Thin Solid Films*, 1992, **216**, 84.
21 L. Niinistö, M. Ritala and M. Leskelä, *Mater. Sci. Eng.*, 1996, **B41**, 23.
22 L. Niinistö, *Proc. Int. Semicond. Conf. CAS*, 2000, **1**, 33.
23 C. Dücsö, N. Q. Khanh, Z. Horváth, I. Barsony, M. Utriainen, S. Lehto, M. Nieminen and L. Niinistö, *J. Electrochem. Soc.*, 1996, **143**, 683.
24 M. Ritala, M. Leskelä, J.-P. Dekker, C. Mutsaers, P. J. Soininen and J. Skarp, *Chem. Vap. Deposition*, 1999, **5**, 7.
25 M. Vehkamäki, T. Hatanpää, T. Hänninen, M. Ritala and M. Leskelä, *Electrochem. Solid State Lett.*, 1999, **2**, 504.
26 H. Seim, H. Mölsä, M. Nieminen, H. Fjellvåg and L. Niinistö, *J. Mater. Chem.*, 1997, **7**, 449.
27 H. Seim, M. Nieminen, L. Niinistö, H. Fjellvåg and L-S. Johansson, *Appl. Surf. Sci.*, 1997, **112**, 243.
28 O. Nilsen, M. Peussa, H. Fjellvåg, L. Niinistö and A. Kjekshus, *J. Mater. Chem.*, 1999, **9**, 1781.
29 M. Schuisky, K. Kukli, M. Ritala, A. Hårsta and M. Leskelä, *Chem. Vap. Deposition*, 2000, **6**, 139.
30 K. J. Eisentraut and R. E. Sievers, *J. Am. Chem. Soc.*, 1965, **87**, 5256.
31 M. Putkonen, L-S. Johansson, E. Rauhala and L. Niinistö, *J. Mater. Chem.*, 1999, **9**, 2449.
32 M. Putkonen, T. Sajavaara and L. Niinistö, *J. Mater. Chem.*, 2000, **10**, 1857.
33 M. Ylilammi and T. Ranta-aho, *Thin Solid Films*, 1993, **232**, 56.
34 S. Geller and V. B. Bala, *Acta Crystallogr.*, 1956, **9**, 1019.
35 *UniQuant Version 2 User Manual*, Omega Data Systems, Neptunus 2, NL-5505 Veldhoven, The Netherlands, 1994.
36 *Axis 165, Operating Manual and User's Guide*, Kratos Analytical Ltd, Manchester, 1995.
37 M. Nieminen, M. Putkonen and L. Niinistö, *Appl. Surf. Sci.*, 2001, **174**, 155.
38 M. Nieminen, L. Niinistö and E. Rauhala, *J. Mater. Chem.*, 1996, **6**, 27.
39 M. Putkonen, T. Sajavaara, L-S. Johansson and L. Niinistö, *Chem. Vap. Deposition*, 2000, **7**, 44.
40 Helsinki University of Technology internal database, unpublished
41 S. Tougaard and A. Ignatiev, *Surf. Sci.*, 1983, **129**, 355.
42 P. A. W. van der Heide and J. W. Rabalais, *Chem. Phys. Lett.*, 1998, **297**, 350.
43 C.-M. Pradier, C. Hinnen, K. Jansson, L. Dahl, M. Nygren and A. Flodström, *J. Mater. Sci.*, 1998, **33**, 3187.
44 P. Burroughs, A. Hamnett, A. F. Orchard and G. Thornton, *J. Chem. Soc., Dalton Trans.*, 1976, 1686.
45 M. Nieminen, S. Lehto and L. Niinistö, *J. Mater. Chem.*, submitted.
46 H. Yamane, K. Ogawara, M. Omori and T. Hirai, *J. Am. Ceram. Soc.*, 1995, **78**, 2385.
47 J. Dohrup, A. Høyvald, G. Mogensen, C. J. H. Jacobsen and J. Villadsen, *J. Am. Ceram. Soc.*, 1996, **79**, 2959.